REPORT DOCUMENTATION PAGE

Form Approved
OMB No. 0704-0188

1. REPORT DATE *(DD-MM-YYYY)* 16-09-2002	**2. REPORT TYPE** Article in Conference Proceeding	**3. DATES COVERED** *(From - To)* 1 Jan 2002 – 31 Jul 2002

4. TITLE AND SUBTITLE
Systematic Effects in Color Photometry Data

5a. CONTRACT NUMBER
F29601-00-D-0204

5b. GRANT NUMBER
N/A

5c. PROGRAM ELEMENT NUMBER
63444F

6. AUTHOR(S)
K. Kim Luu, Capt Josh Snodgrass, Chris Sabol, John Lambert, Kris Hamada

S. Maile Giffin

5d. PROJECT NUMBER
4868/4983

5e. TASK NUMBER
B3

5f. WORK UNIT NUMBER
BH

7. PERFORMING ORGANIZATION NAME(S) AND ADDRESS(ES)

AFRL/DEBI (Det 15)
535 Lipoa Parkway Ste 200
Kihei HI 96753

8. PERFORMING ORGANIZATION REPORT NUMBER

Det 15 AFRL 0234

9. SPONSORING / MONITORING AGENCY NAME(S) AND ADDRESS(ES)

10. SPONSOR/MONITOR'S ACRONYM(S)

11. SPONSOR/MONITOR'S REPORT NUMBER(S)

12. DISTRIBUTION / AVAILABILITY STATEMENT
Approved for public release; distribution is unlimited.

13. SUPPLEMENTARY NOTES
K. Luu, J. Lambert, K. Hamada, J. Snodgrass, C. Sabol, and M. Giffin, "Systematic Effects in Color Photometry Data," 2002 AMOS Technical Conference, Maui, Hawaii, 16-20 September 2002.

14. ABSTRACT
Previous work with laboratory and field observations and computer simulations suggests that classes of spacecraft can be distinguished on the basis of their color or spectral properties. Empirical results also indicate that accounting for systematic effects reduces much of the observed scatter and thus increases separability of the classes. We seek to gain an understanding of the basic properties of satellite features that determine the spectral characteristics of individual satellites: surface materials and scattering properties, combination of materials, shape, orientation, illumination-viewing geometries, etc. Initial efforts have focused on systematic effects of solar phase angle on the object brightness and color data.

20040324 057

15. SUBJECT TERMS

Satellites, color photometry data

16. SECURITY CLASSIFICATION OF:			**17. LIMITATION OF ABSTRACT**	**18. NUMBER OF PAGES**	**19a. NAME OF RESPONSIBLE PERSON** K. Kim Luu
a. REPORT Unclassified	**b. ABSTRACT** Unclassified	**c. THIS PAGE** Unclassified	UNLIMITED	11	**19b. TELEPHONE NUMBER** *(include area code)* (808) 874-1608

SYSTEMATIC EFFECTS IN COLOR PHOTOMETRY DATA

K. Kim Luu, Capt. Joshua Snodgrass, Chris Sabol
Air Force Research Lab, Directed Energy Directorate, 535 Lipoa Parkway, Suite 200, Kihei, HI 96753

John V. Lambert, Kris Hamada
Boeing LTS, 535 Lipoa Parkway, Suite 200, Kihei, HI 96753

S. Maile Giffin
Oceanit, 590 Lipoa Parkway, Suite 264, Kihei, HI 96753

ABSTRACT

Previous work with laboratory and field observations and computer simulations suggests that classes of spacecraft can be distinguished on the basis of their color or spectral properties. Empirical results also indicate that accounting for systematic effects reduces much of the observed scatter and thus increases separability of the classes. We seek to gain an understanding of the basic properties of satellite features that determine the spectral characteristics of individual satellites: surface materials and scattering properties, combination of materials, shape, orientation, illumination-viewing geometries, etc. Initial efforts have focused on systematic effects of solar phase angle on object brightness and color data.

1. BACKGROUND

For the purpose of identifying and characterizing satellites in Earth orbit, ground-based optical telescopes are employed with both imaging and nonimaging sensors. Many satellites of interest are unresolved or poorly-resolved due to their small size and/or long range from the observing station. For these situations, nonimaging techniques are viable avenues to gather information essential for target identification, characterization of status and function, and in some cases, anomaly resolution. Even for the case of well-resolved objects, nonimaging techniques can provide additional and complementary data to provide a more complete characterization of the objects. These techniques include photometry, radiometry, spectroscopy, polarimetry and vibrometry. Analysis of the data is not generally straightforward, however. Optical characteristics of individual satellites are influenced by a wide variety of parameters, such as surface scattering properties, material composition, shape, orientation, and illumination and viewing geometries. In this situation, the inverse problem is to associate key observables with the distinguishing physical characteristics of an individual spacecraft or a defined satellite class. In order to determine the fundamental limitations of the inverse problem, the direct problem must be addressed first. Hence, an understanding of the basic properties that influence spectral and polarimetric characteristics is sought.

Preliminary efforts in this study have focused on color photometry data. The difference of magnitudes in any two spectral bands defines a color, which represents the ratio of flux between the two bands. The magnitude scale is the same logarithmic scale used by astronomers, with larger values of magnitude denoting dimmer objects and a difference of 1 magnitude representing a luminous flux (i.e., brightness) ratio equal to the fifth root of 100 (approximately 2.51). Color indices are generally expressed as the "bluer" band minus the "redder" band so that larger values of color indices denote redder colors. Under passive illumination conditions, satellite color indices are the color indices of the Sun modified by scattering and spectral properties of the combination of surface materials. Colors also vary with satellite orientation and viewing and illumination geometries as various surface features are exposed or hidden. In common use are the standard Johnson broadband filters, the characteristics of which are plotted in Fig. 1. Since this system was tuned specifically for spectral measurements of astronomical objects, efforts have been made under the Air Force Space Battlelab's Space Object Identification In Living Color (SILC) initiative to define a new set of spectral bands that may be more effective for satellite discrimination [1]. The effectiveness of the SILC filters is discussed in [2] and demonstrates a better performance in object discrimination than the Johnson filters in some instances, though ambiguity among objects of different classes still exists.

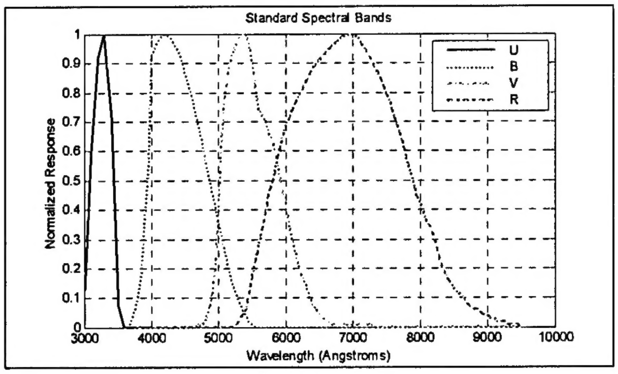

Fig. 1. Normalized Spectral Responses of the Standard U, B, V, and R Pass Bands

Expected variations in satellite colors can be estimated through analytical models and computer simulation. A past study utilized a simple mathematical model to examine color differences of two common surface materials, solar cells and gold foil. It concluded that the differences should be detectable by current systems and may be sufficient to support class recognition and orientation monitoring [3]. More detailed simulations involved precise three-dimensional models of actual spacecraft with the optical properties represented by laboratory measurements of bi-directional reflectance functions (BDRF) of satellite materials [4]. Color indices for a number of satellite classes were computed for various illumination and viewing geometries and spacecraft orientations. Results indicate that for many cases the color indices can be used to discriminate between the classes and furthermore, to detect changes from nominal orientations. These studies focused on satellites in geosynchronous Earth orbits (GEO). In low Earth orbits (LEO), the situation for the poorly-resolved microsatellite class and smaller spacecraft presents additional challenges arising from infrequent observation opportunities, shorter terminator conditions (i.e., the time during which the satellite is sun-illuminated but the observation station is in darkness), and larger and more rapid changes in orientation angles. Preliminary analyses indicate that photometric integration times can be adjusted to capture sufficient signal while balanced with changing orientation angles. Beyond addressing feasibility issues, simulations can also be employed to gain insight into the fundamental relationships between optical properties and key influencing parameters. One part of this work aims to uncover these relationships; preliminary efforts are discussed in following sections.

Analyses of field data demonstrate that certain spacecraft classes can be distinguished based on color photometry measurements [3]. However, considerable overlap in the observed colors appeared due to systematic effects related to illumination and viewing geometries in addition to noise in the measurement process. Fig. 2a is a color-color plot of observed B-V (Blue-Visible) and V-R (Visible-Red) colors for 25 spacecraft based on data collected by W.I. Beavers et al. at MIT/Lincoln Laboratory ETS optical site near Socorro, NM, during 1988-90 [5]. A data point at 0-0 on this plot represents a "colorless" object, with equal brightness in the several spectral bands. Also shown are the color values for the Sun. In general, the satellite colors tend to be redder than the Sun. Although there is some clustering of the observations for individual satellites, there is considerable scatter in the observations and the clusters overlap. These effects are better shown in Fig. 2b where the means and standard deviations of the observed colors for each satellite have been plotted. The scatter in the observations is larger than would be expected from measurement uncertainties alone and are suspected to be the result of systematic effects. An objective of this study is to obtain a better understanding of the processes that produce the observed satellite colors with a goal of being able to remove the systematic effects. The corrected satellite colors may then be able to provide information on the satellite configuration and may provide a technique for rapidly distinguishing between classes of spacecraft.

Other studies have explored pattern recognition approaches to discriminate between object classes despite significant overlap in observed colors. In [6], the results from application of three variations of statistical classifiers (K-nearest neighbor, Gaussian, and Mahalanobis distance) are discussed. The Mahalanobis distance classifier performed the best in correctly identifying the objects by type of platform (Hughes 601, GE Satcom 5K, and LMAS 3000); it was successful in 86% of the cases. In the more stringent test of identifying the type of satellite (Solidaridad, DBS, AMSC, Anik, and Gstar/Spacenet), the success rate fell to 55%. If systematic effects could be removed, the success rate may be significantly improved. Additionally, the class sizes could be further reduced so that more information may be gleaned from the data.

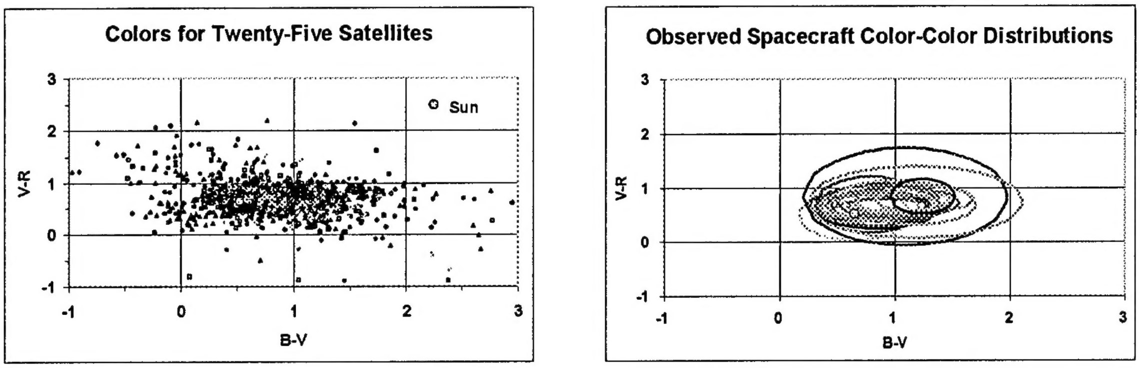

Fig. 2. a). Color-Color Plot for 25 Spacecraft and b). Statistical Distribution of Colors for 25 Spacecraft

Ultimately to separate spacecraft of similar colors, other techniques which examine different optical properties, such as polarimetry, will be required. Previously, analysis of simulated active and passive polarization signatures using the Time-domain Analysis Simulation for Advanced Tracking (TASAT) software indicated some potential capability for satellite discrimination, though the results were dependent on the accuracy of the TASAT materials database and polarization rendering capabilities [7]. With passive (i.e., solar) observation of both GEO and LEO spacecraft, variations in the Stokes parameters and degree-of-polarization are useful discriminators. While initial efforts in this study focused on color photometry, future work will certainly include other nonimaging techniques.

2. NORMALIZATION OF OPTICAL SIGNATURES

As discussed in the previous section, the observational color photometry data for satellites are scattered due to both systematic effects and measurement uncertainties. The latter category encompasses anything related to the measurement process that introduces variations in the brightness not due to the target itself and includes detector photon statistics, detector noise, atmospheric variations, and uncertainties in the calibration. On the other hand, systematic effects are introduced by variations in such factors as solar phase angle, solar declination, satellite orientation, and target range over different observations. The resulting overlap in observed colors for different satellite classes introduces significant ambiguity into object identification and characterization efforts.

Observation data are frequently corrected or normalized to remove known and well-understood effects such as range, atmospheric extinction, and sensor nonlinearities. By removing these effects from optical signatures, the observables related to the intrinsic properties of the target spacecraft become more apparent, and data collected at different times or on different objects can be directly compared. In the example shown in Fig. 3, the observed brightness of a satellite, shown as a function of time during an observing pass with time zero corresponding to the time of culmination (i.e., at maximum elevation angle and minimum range), is simulated. The apparent or observed brightness of the satellite displays considerable variation during the pass, making it difficult to determine the spacecraft configuration, surface properties, and dynamics. When the signature is normalized to a standard range, the absolute brightness is shown to be constant throughout the pass, indicating that the target may be a homogeneous sphere. In the same way, it is expected that when systematic effects in satellite color data are removed, the corrected colors will be more indicative of their intrinsic properties and less affected by the observing conditions. This would allow better determination of the satellite's physical characteristics and make the differences between spacecraft types more evident.

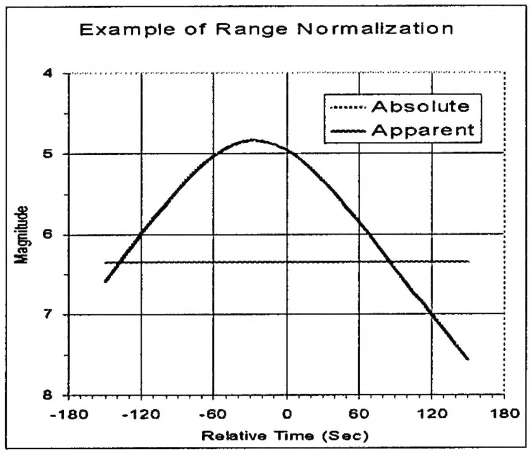

Fig. 3. Range Normalization

Observers have long noted that satellites tend to become bluer as their brightness increases. This effect is generally attributed to increasing contributions to the total satellite brightness by the "blue" solar panels, occurring at low phase angles when the specular glint from the panels can be observed. Trends in color as a function of brightness have also been observed for satellites that have no solar panels, such as rocket bodies, indicating that the effect can be produced by other types of surfaces. A better understanding of the sources of the observed satellite colors and changes in colors necessitates a detailed study of the spectral and scattering properties of all types of satellite surfaces and satellite configurations.

Fig. 4 illustrates the observed change in spacecraft color with brightness. The plot shows the observed B-V and V-R colors for three Intelsat satellites plotted as a function of the observed V-band magnitude. The total brightness of the spacecraft increases as the magnitude decreases in value, and the color becomes bluer as the color value decreases. Thus, Fig. 4 shows that the Intelsat spacecraft become bluer as the brightness increases. To first order, the trend appears to be linear. The scatter in the observations about the fitted line is still greater than expected from the measurement uncertainties alone and may indicate that the relationship is not strictly linear or that other factors, such as the illumination geometry, may also be introducing systematic effects. It is also possible that differences between individual spacecraft of the same type may be present. All of theses factors are being examined.

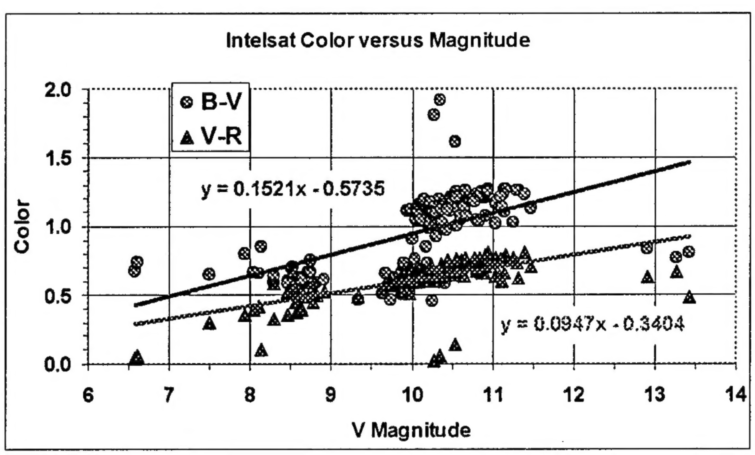

Fig. 4. Magnitude Normalization of Colors

As a first step towards reducing scatter in the observations and improving the separability of spacecraft types, the effect of removing the linear trend in color as a function of brightness is examined. The data comes from an extensive set of observational color data on spacecraft that was collected under a program headed by W.I. Beavers of MIT Lincoln Laboratory. Thousands of individual brightness, color, and polarization measurements were made between 1987 and 1995 on over one hundred satellites. These observations were published in three reports [5,8,9]. The first report contains 1,819 sets of V magnitude and two color (B-V and V-R) observations for 66 cataloged objects. The original data listings contain over 3,300 measurement sets. Several of the data sets are incomplete, containing only magnitudes or one color. Examination of the entire data ensemble shows a concentration of points between B-V values of 0 and +2 and between V-R values of 0 and +1, with no obvious clustering that might be related to specific objects or spacecraft classes. The wider dispersion in B-V than V-R is consistent with modeled color results for typical spacecraft materials. The standard deviations for the averages are large, averaging 0.45 magnitudes for B-V and 0.33 magnitudes for V-R. As noted in the report, there were large night-to-night variations in the calibration parameters, especially in the zero point, which should have remained constant over long periods of time. The data is estimated to be accurate to 0.2-0.3 magnitudes.

Thirty-one identified satellites with at least 20 observation sets each were selected for detailed analysis. The measured colors were normalized to their estimated value at a standard magnitude by projecting them along a line parallel to the line fitted to all of the observations for that color. Fig. 5 demonstrates the effects of normalization by magnitude by plotting the statistical distributions of the individual satellites before and after normalization. Color distinctions between objects are more obvious, though overlaps are still present in many cases. When the class definitions are broadened from individual satellites to groups of common satellite platforms, even more separation is achieved, as seen in Fig. 6. This represents a tradeoff between confidence in accurate classification and quality of the information obtained. It is important to note that the results are sensitive to the choice of the standard magnitude. For example, choosing a standard magnitude too close to the observed magnitudes de-emphasizes the significance of the slope of the fitted line, while choosing a standard magnitude too far away over-emphasizes the effect of the slope. For observations of GEO satellites, which tend to have observed magnitudes around tenth visual magnitude, a standard magnitude of zero appears to be a reasonable choice. It has the added advantage that the mean of the normalized color distribution is equal to the intercept of the fitted line.

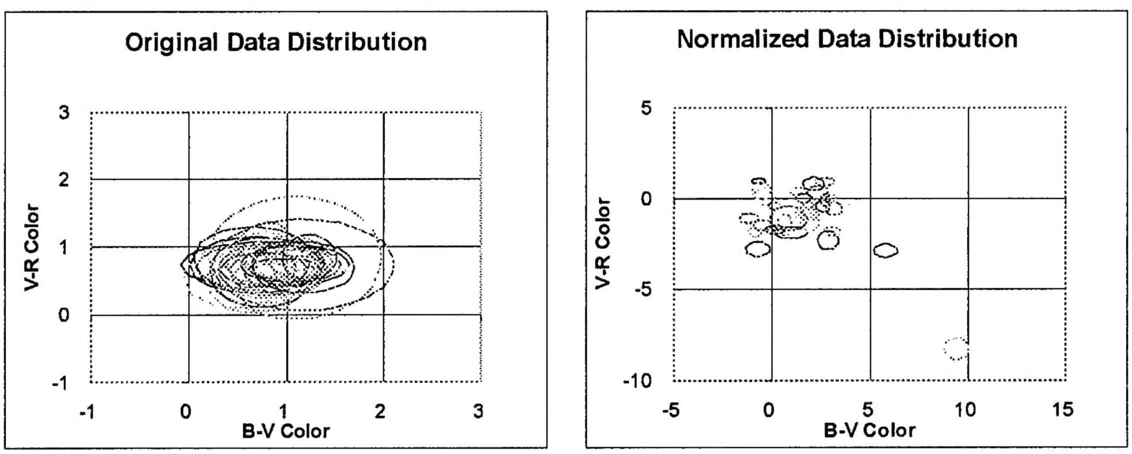

Fig. 5. a). Original Statistical Distribution of 31 Satellites and b). Distribution of 31 Satellites After Normalization by Magnitude

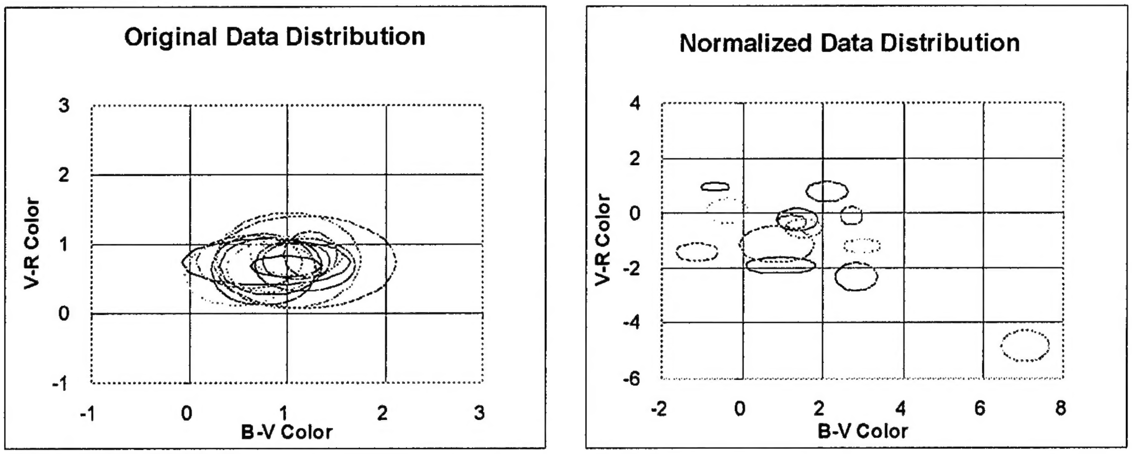

Fig. 6. a). Original Statistical Distribution of 13 Satellite Groups and b). Distribution of 13 Satellite Groups After Normalization by Magnitude

Using the same data set, normalization by solar phase angle was explored next. The relationship between color and phase was also assumed to be linear in a first order approximation. Interestingly, the 31 individual objects showed little if any trend for separation after normalization at zero phase (Fig. 7a) in comparison with the original statistical distribution (Fig. 5a). With the normalization standard shifted to 90°, two objects are seen to pull away (Fig. 7b). A plausible explanation for the behavior of those two particular objects lies in the fact that they lack solar panels and are the only ones that are so configured. However, the puzzle here centers about the apparent similarity in color of spinning and 3-axis stabilized spacecraft, both of which are amply represented in the analysis. At 90° phase, the solar panels of functioning 3-axis stabilized spacecraft should appear edge-on to the observer so that the spacecraft body dominates its color; while at 0° phase, with the panels squarely facing the observer, the color results from a combination of the panels and the body. Spinning spacecraft on the other hand presumably display little color differences over changing phase angles. This expected difference in color did not materialize in the results.

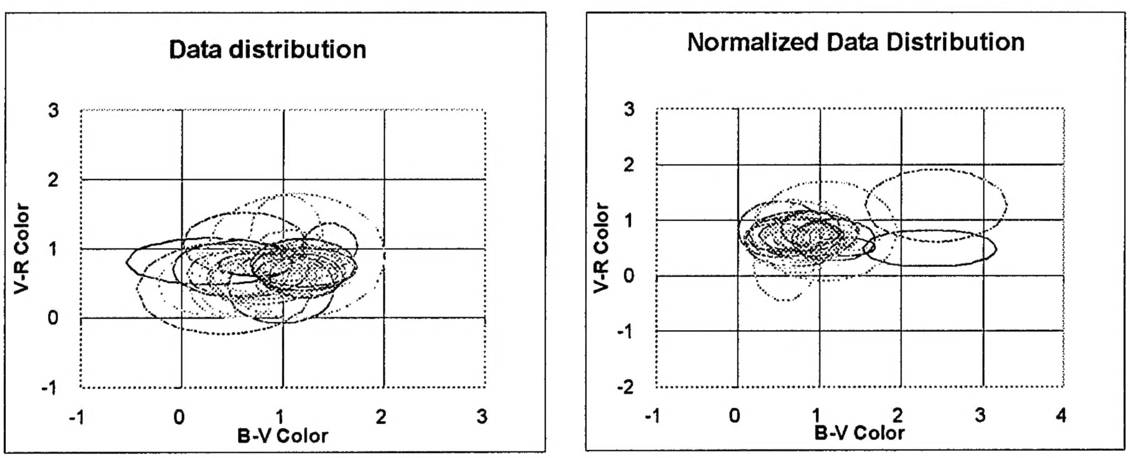

Fig. 7. a). Distribution of 31 Satellites After Normalization at 0° Phase Angle and b). Distribution of 31 Satellites After Normalization at 90° Phase Angle

This difference between phase and brightness normalization techniques is partially explained by Fig. 8. The results of a simulation illustrate the behavior of visual magnitude as a function of phase angle for a space-based observer (SBV) and a ground-based observer (Gnd). The relationship is roughly linear above 30° phase. With smaller phases, the SBV measures large scattering while the ground-based observer sees a decidedly nonlinear trend. More

in-depth studies are required to provide a complete understanding of this issue as well as others presented by this analysis. In Fig. 6b, 5 groups of satellites remain overlapped, but it is uncertain if these objects are truly similar in color or perhaps other significant systematic effects are present. Another question is whether normalization with a linear function is most appropriate. To approach the common underlying puzzle, surface scattering properties of surface materials are examined.

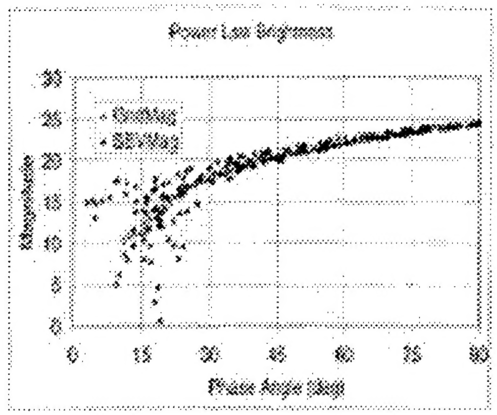

Fig. 8. Relationship Between Visual Magnitude and Phase Angle

3. SURFACE SCATTERING PROPERTIES

To achieve an in-depth understanding of satellite signatures, models are being developed that begin at the microscopic level describing the interaction of light with the individual types of surfaces (i.e., metals, paints, solar cells, etc.) to obtain the directional, spectral, and polarization properties of the scattered light. These surface models are then combined to represent the larger structures to obtain the macroscopic optical signatures of the spacecraft. The surface models include the results of laboratory measurements of pristine materials but also incorporate space weathering and other effects that modify the optical surface properties of actual on-orbit spacecraft [10].

Generally, two components of scattering caused by light hitting a material surface are considered. The specular component is a surface reflection. In this model, light from each incoming ray reflects in one direction only, with the incident angle of the light rays equal to the reflection angle. Specular reflections are bright and are significantly influenced by small changes in angle between the illumination source, the object, and the observer. Because a specular reflection originates from the surface of the object and does not undergo multiple internal reflections, it maintains its polarization direction. For slightly rough surfaces, specular reflections are concentrated in a compact lobe around the specular direction. The diffuse component is the result of light rays penetrating the surface, undergoing multiple internal reflections, and re-emerging through the surface. The distribution is shown as a wide range of directions centered around the normal to the surface. Diffuse reflections are randomly polarized. In reality, objects exhibit a range of behaviors from the extreme specular to diffuse.

An example of the modeling at this level includes development of a model to describe the BDRF of a solar cell. Solar cells are fairly complex multi-layered surfaces consisting of a variety of materials. Reflection and scattering occurs from and within each of these layers and affects the properties of the scattered light. Fig. 9 shows a laboratory measurement of a BDRF for a typical solar cell using a logarithmic intensity scale [11]. While the scattering is primarily specular or mirror-like, there is low-level, diffuse structure that will contribute to a satellite's signature at off-specular conditions. This diffuse feature arises from surface imperfections, inclusions, contamination, and other sources that need to be modeled. As the surface weathers in space, this diffuse component increases. A Monte-Carlo simulation is being developed to model the interaction of light with the solar cell layers at the individual photon level to develop functions that will accurately describe the BDRFs and other optical properties.

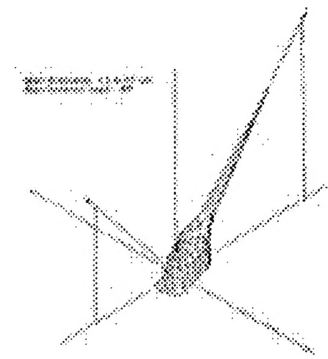

Fig. 9. Solar Cell BDRF

Similar models are being developed for painted surfaces, which are also optically complex structures consisting of particulate pigments suspended in a semi-transparent binder. Space weathering of painted surfaces is especially significant, resulting in rapid color changes and long-term loss of the binder or "chalking" [10]. Scattering models for metallic surfaces will be based on available theoretical and laboratory results but will also include the effects of machining and weathering. The surface models are being developed as modules so that simple models can initially be included and later replaced with more detailed representations.

The optical scattering models for the individual types of surface components are then combined to represent major spacecraft components such as solar panels, body structures, and antenna arrays. Assembly practices, manufacturing tolerances, flexure, and other effects must be considered in computing the detailed optical scattering from these components. Occasionally, for example, solar panels have been modeled using the optical properties for a single solar cell, resulting in unrealistically narrow specular lobes in the computed signatures. In practice, when individual solar cells are assembled into a panel the individual surface normals are not exactly aligned. Fig. 10a shows the measured orientations for the solar cell surface normals for a production spacecraft solar panel sub-array [11]. When the BDRFs for individual solar cells are summed to form an array with this normal orientation distribution, a much broader solar cell array BDRF is obtained as indicated in Fig. 10b, in which a single solar cell BDRF is shown with a different intensity scale for comparison [12]. Solar panel sub-arrays can be positioned at different angular orientations and aligned in different directions so that the panel BDRF contains multiple glint lobes. Other solar panel components such as support structures and frames, and thermal control surfaces, also contribute to the overall signature creating a very complex reflectance function, which has wide variations in intensity, polarization, and color at different illumination, and viewing geometries.

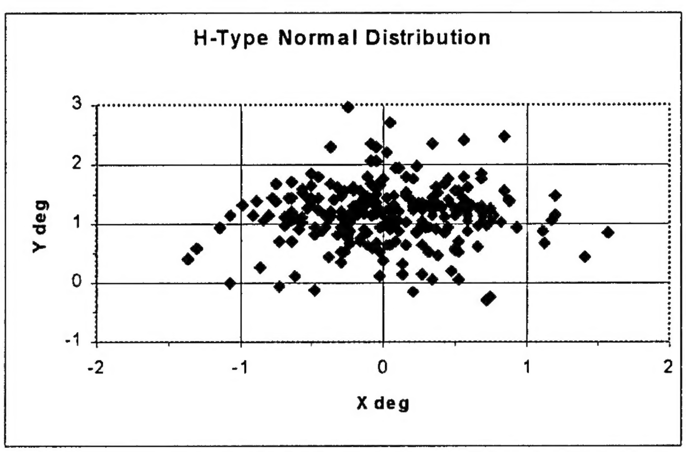

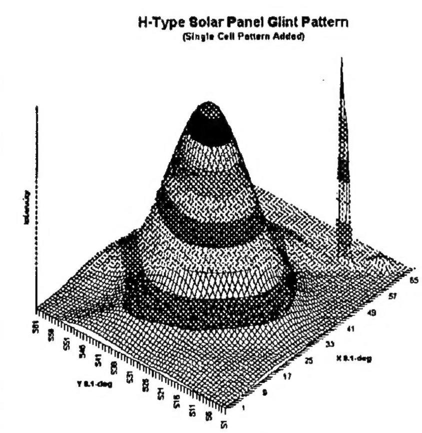

Fig. 10. a). Measured Solar Cell Surface Normal Distributions for a Production Solar Panel and b). the Resulting Panel BDRF (Compared to an Individual Solar Cell BDRF

An optical model for an entire spacecraft is then created by combining the models for the components. Modeling the total optical scattering from a spacecraft takes into account the orientation and orbital motion of the spacecraft, observer and sun positions, and relative motions of sun-tracking solar panels to obtain the composite signature. Initially the spacecraft models are only considering the largest components, such as the body and solar panels, to provide insight into general behavior of the signature as their relative contributions vary with the changing illumination geometry. An example of one of these models consists of a nadir-pointing cylindrical body with a front mounted antenna array and sun-tracking solar panels, as shown in Fig. 11a. The contributions of the individual components can be summed throughout the pass in order to calculate the variations in total intensity, color, and polarization. A signature computed for this model is shown in Fig. 16 as a function of phase angle.

Even at this simple level, the models are providing significant insights into the systematic variations in spacecraft optical signatures. For example, Fig. 11b highlights an asymmetry with respect to minimum phase angle that should be expected for many satellites (an exception would be a geostationary satellite at the same longitude as the observer). This asymmetry arises as a result of the observer viewing a larger fraction of the satellite's Sun-illuminated surfaces either before or after minimum phase, depending on the viewing-illumination geometry. Therefore photometry analyses should not just look at the absolute value of phase angle when comparing different observations but should account for this potential asymmetry. As the understanding of the signatures evolves, other components and more detailed scattering functions will be added to the spacecraft model to improve the fidelity of the simulations.

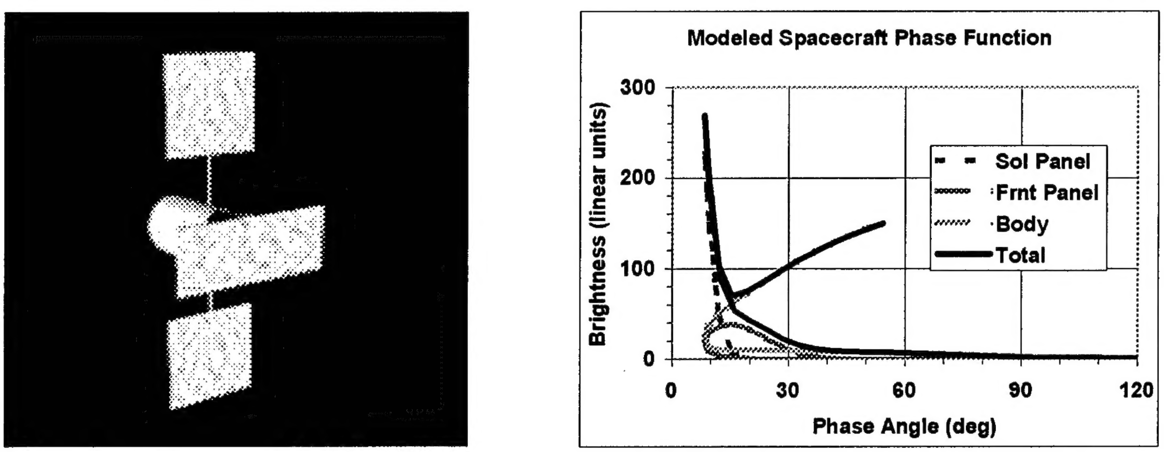

Fig. 11. a). Simple Spacecraft Model Example and b). Simulated Spacecraft Intensity Signature Showing Component Contributions

4. CONCLUSION

Much can be learned about space objects from color photometry measurements. However, observational and systematic effects significantly complicate the problem, making direct comparison of various observations nearly meaningless. By accounting for these known factors, observation data can be analyzed to provide more accurate, descriptive, and useful information. More work is required to develop a full understand of these effects, but it is clear that application of various normalization techniques is critical to rigorously characterizing space objects.

Future efforts will focus on developing the optical scattering model to gain an in-depth understanding of satellite signatures. Scattering functions associated with common spacecraft materials will be sought to create additional modules. Directional, spectral, and polarization properties will all be examined, as the study expands beyond color photometry techniques.

5. ACKNOWLEDGMENTS

This work was funded by the Air Force Office of Scientific Research, Directorate of Mathematics and Space Sciences. The authors would like to give thanks especially to Dr. Clifford Rhoades, Maj. William Hilbun, and Dr. Charles Matson for their encouragement and support.

6. REFERENCES

1. Talent, D.L., Sydney, P., et al., *The Space Battlelab Space Object Identification In-Living Color (SILC) Final Report*, February 2000.
2. Payne, T.E., Gregory, S.A., et al., "Color Photometry of Geosynchronous Satellites Using the SILC Filters," *Proceedings of the Symposium on Optical Science and Technology*, SPIE 46th Annual Meeting, 2001.
3. Lambert, J.V., *Operational Utility of Multicolor Photometric Measurements*, Maui Space Surveillance System Specialized Data Report, MSSS FY97-01, August 1997.
4. Payne, T.E., *Spectral Photometry Study for Deep Space SOI*, Final Report Contract SDIO84-92-C-0008, Schafer Corporation, August 1997.
5. Beavers, W.I., Cho, J.Y., et al., *Satellite Multicolor Photometry*, Project Report STK-229, MIT Lincoln Laboratory, December 1994.
6. Payne, T.E., Gregory, S.A., et al., "Space Object Identification of Geosynchronous Satellites," *Proceedings of the 1999 AMOS Technical Conference*, Maui, Hawaii, August-September 1999, pp. 195-203.
7. Bush, K.A., Crockett, G.A., et al., "Satellite Discrimination From Active and Passive Polarization Signatures: Simulation Predictions Using the TASAT Satellite Model," *Proceedings of SPIE*, Vol. 4481, January 2002, pp. 46-57.
8. Beavers, W.I. and Swezey, L.W., *Optical Monitoring of Geosynchronous Satellites Final Report*, Project Report STK-240, MIT Lincoln Laboratory, October 1995.
9. Beavers, W.I., *UBV Photometry of Geosynchronous Satellites*, Project Report STK-241, MIT Lincoln Laboratory, October 1995.
10. Culp, R.D.; Jorgensen, K., et al., "Use of Optical Characteristics to Identify Orbiting Material," *Space Debris Journal*, Kluwer Academic Publishers, Netherlands, 2000.
11. Bair, M.E, Carmer, D., et al., *Determination of Satellite Observables Study, Volume IV, Optical Properties of Satellite Materials*, SAMSO TR 73-291, Air Force Space and Missile Organization, May 1974.
12. Kervin, P.; Africano, J.; et al., "A Search for the Lost IDSCP Constellation," *Proceedings of the 2001 Space Control Workshop*, MIT Lincoln Laboratory, April 2001.